Phytochemistry 214 (2023) 113830

Contents lists available at ScienceDirect

Phytochemistry

journal homepage: www.elsevier.com/locate/phytochem

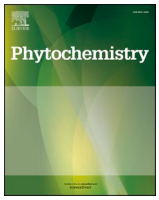

Steccherins A–D, chamigrane-type sesquiterpenes from the fungus *Steccherinum ochraceum* with selective inhibition on B lymphocyte proliferation

Shan-Shan Huang [a], Hui-Xiang Yang [a], Juan He [a], Bing-Chao Yan [b], Tao Feng [a,*], Ji-Kai Liu [a,**]

[a] School of Pharmaceutical Sciences, South-Central Minzu University, Wuhan, 430074, China
[b] State Key Laboratory of Phytochemistry and Plant Resources in West China, Kunming Institute of Botany, Chinese Academy of Sciences, Kunming, 650201, China

ARTICLE INFO

Keywords:
Steccherinum ochraceum
Chamigrane sesquiterpenes
Steccherins A–D
Immunosuppressive activity

ABSTRACT

Four previously undescribed chamigrane sesquiterpenes, namely steccherins A–D, have been isolated from the fungus *Steccherinum ochraceum.* Their structures were elucidated by extensive spectroscopic analysis, as well as computational methods and single crystal X-ray diffraction. Steccherins A and B possess previously undescribed backbones which might be derived from normal chamigrane sesquiterpenes, especially that steccherin A possesses a spiro[5.6]dodecane carbon skeleton via a ring-rearrangement. Steccherins A, C, and D showed immunosuppressive activity with IC_{50} values ranging from 6.2 to 37.8 μM. The data suggested that these chamigrane sesquiterpenes have potential selective inhibition on LPS-induced B lymphocyte proliferation.

1. Introduction

Fungi inhabit almost all known ecosystems on Earth (Grossart et al., 2019). Over hundreds of millions of years of co-evolution with their hosts, fungi have built up the ability to produce a complex array of secondary metabolites that often have important biological functions (Conrado et al., 2022; Pusztahelyi et al., 2015; Rustamova et al., 2020; Singh et al., 2021). Penicillin, cyclosporin A, lovastatin, myriocin, mycophenolic acid and other famous fungal natural drugs play an irreplaceable role in antimicrobe, immunosuppression, cardiovascular and cerebrovascular diseases and other aspects (Hridoy et al., 2022; Hyde et al., 2019; Ortega et al., 2021; Wang et al., 2022). With the in-depth development of biosynthesis of fungal products and the exploration of key enzyme functions, the discovery of novel fungal natural products has been greatly promoted, and the clinical application prospect of fungal natural products has been further enhanced.

Autoimmune diseases pose a long-term threat to human health, and some malignant diseases such as lupus erythematosus and ankylosing spondylitis are still intractable medical problems (Edner et al., 2020; Ramalingam and Shah, 2021; Rose, 2016). Therefore, it is very important to find new immunosuppressive agents. Our previous studies have shown that fungal sesquiterpenes have certain immunosuppressive activities, especially some of them show selective inhibition on B lymphocytes. For instance, antroxazole A and antrodillin are two sesquiterpenes from *Antrodiella albocinnamomea* that possesses selective inhibitory activity against the LPS-induced proliferation of B lymphocytes with IC_{50} values of 16.3 and 6.6 μM, respectively (He et al., 2022; Liang et al., 2021), while tremutins A and B are two sesquiterpenes from *Irpex lacteus* which also show inhibitions on B cell proliferation with IC_{50} values of 22.4 and 13.6 μM, respectively (Wang et al., 2020). The discovery of these molecules opened up a breakthrough in the search for new immunosuppressive agents.

Steccherinum ochraceum (Pers.:Fr.) Gray. (Hydnaceae) is a white rot basidiomycete fungus occurring throughout the world. It grows on fallen wood of broadleaf trees and participates in wood degradation and soil organic matter decomposition (Moiseenko et al., 2019). Previous chemical studies on this fungus have demonstrated the presence of chamigrane-type sesquiterpenes (Liu et al., 2010; Liu and Luo, 2010; Zhao et al., 2019, 2021). In order to search for more active metabolites, the chemical constituents of *S. ochraceumi* cultured in rice medium were studied. As a result, four chamigrane sesquiterpenes, namely steccherins A–D (**1**–**4**, Fig. 1), have been isolated. The structures were established by means of spectroscopic methods, single-crystal X-ray diffraction, and computer calculations. All compounds were evaluated for their

* Corresponding author.
** Corresponding author.
E-mail addresses: tfeng@mail.scuec.edu.cn (T. Feng), liujikai@mail.scuec.edu.cn (J.-K. Liu).

https://doi.org/10.1016/j.phytochem.2023.113830
Received 22 May 2023; Received in revised form 16 August 2023; Accepted 17 August 2023
Available online 18 August 2023

immunosuppressive activity. Herein, the separation, structure elucidation, and bioactivity of these isolates are reported.

2. Results and discussion

Compound 1 was obtained as a colorless oil. Its molecular formula $C_{15}H_{22}O_3$ was determined by HRESIMS (measured at *m/z* 251.16414 $[M + H]^+$; calcd for $C_{15}H_{23}O_3^+$, 251.16417), corresponding to five degrees of unsaturation. The ^{1}H NMR spectrum of 1 exhibited two singlets for methyl groups at δ_H 0.86 and 0.89, and three olefinic protons at δ_H 5.06, 5.15 and 5.48. The ^{13}C NMR and DEPT spectra displayed fifteen signals attributing to two CH_3, five CH_2, four CH, and four non-protonated carbons (Table 1). Of them, signals at C-3 (δ_C 72.1), C-2 (δ_C 79.5), and C-15 (δ_C 68.0) were suggested to be attached to oxygen atoms. In addition, four olefinic carbons at C-7 (δ_C 164.3), C-8 (δ_C 95.7), C-9 (δ_C 122.9) and C-10 (δ_C 123.8) were ascribable for two double bonds. These data indicated that 1 should be a tricyclic sesquiterpene. The ^{1}H–^{1}H COSY spectrum established partial structures of H-1/H-2, H_2-4/H_2-5, and H-8/H-9/H-10/H_2-11, as shown in Fig. 2. In the HMBC spectrum (Fig. 2), the correlations from H_3-13 and H_3-14 to C-12, C-6 and C-11 established the connection of C-11/C-12/C-6. In addition, the HMBC correlations from H-8 to C-7 and C-6 established the connection of C-6/C-7/C-8. The above two fragments constructed a seven-membered ring A (Fig. 2). Continuing analysis of HMBC data, the fragments of H-1/H-2 and H_2-4/H_2-5 were connected by C-3 and C-6, as supported by HMBC correlations of H-1, H-2, H-4, H-5 to C-3 and C-6, respectively. Therefore, C-1 to C-6 established one six-membered ring B (Fig. 2). Furthermore, a key HMBC correlation from H-2 to C-7 suggested that an ether bond was established between C-2 and C-7, which constructed a furan C (Fig. 2). Fully analysis of HMBC data indicated that a hydroxymethylene group at C-15. Therefore, compound 1 was established as a tricyclic sesquiterpene possessing a novel 7/6-fused carbon skeleton. In the ROESY spectrum, the cross peaks of H_3-14/H-5a and H-5b/H_2-15 established the relative configuration as shown in Fig. 3. The final structure with absolute configuration was determined by single crystal X-ray diffraction (Fig. 4). Thus, the structure of 1 was established and trivially named as steccherin A.

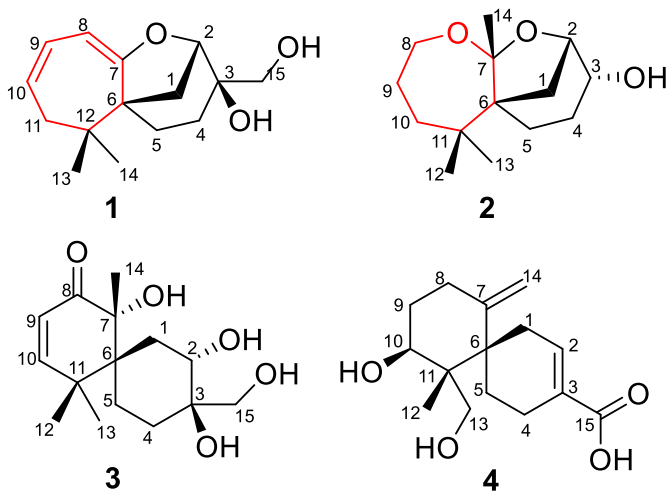

Fig. 1. Chemical structure of compounds 1–4.

Compound 2 was obtained as a colorless oil. Its molecular formula $C_{14}H_{24}O_3$ was determined by HREIMS (measured at *m/z* 240.1728 $[M]^+$; calcd for $C_{14}H_{24}O_3$, 240.1725), corresponding to three degrees of unsaturation. The ^{1}H NMR spectrum of 2 exhibited three singlets for methyl groups at δ_H 0.92, 1.03 and 1.57. The ^{13}C NMR and DEPT spectra had fourteen signals attributable to three CH_3, six CH_2, two CH, and three non-protonated carbons (Table 1). Of them, one signal at δ_C 110.0 was characteristic for an acetal (or a ketal) carbon, while signals at δ_C 71.9, 78.6, and 61.9 should be attached to oxygen atoms. Besides, no double bonds or carbonyl carbon atoms were found. This information suggested that compound 2 should be a tricyclic sesquiterpene. The ^{1}H–^{1}H COSY spectrum of 2 established two partial structures of H_2-1/H-2/H-3/H_2-4/H_2-5 and H_2-8/H_2-9/H_2-10 as shown in Fig. 2. In the HMBC spectrum (Fig. 2), correlations from H_3-12 and H_3-13 to C-10, C-11, and C-6 established the connection of C-6/C-11/C-10, while correlations from H_2-8 to C-7 established an ether bond of C-8–O–C-7. Therefore, an

Table 1
^{1}H and ^{13}C NMR data for compounds 1–4.

No.	1[a]		2[b]		3[a]		4[a]	
	δ_C, type	δ_H (*J* in Hz)	δ_C, type	δ_H (*J* in Hz)	δ_C, type	δ_H (*J* in Hz)	δ_C, type	δ_H (*J* in Hz)
1a	36.1, CH_2	1.99, m	36.4, CH_2	2.67, m	30.4, CH_2	2.15, dd (15.3, 4.4)	31.5, CH_2	2.55, m
1 b				1.21, m		2.02, m		2.30, m
2a	79.5, CH	4.19, d (5.5)	78.6, CH	4.26, d (7.7)	71, CH	3.77, t (5.0)	140.3, CH	6.94, m
2 b								
3	72.1, C		71.9, CH	3.51, t (7.4)	73.8, C		130.7, C	
4a	29.4, CH_2	1.44, dd (12.8, 5.5)	29.9, CH_2	2.09, m	29.7, CH_2	1.99, m	23.00, CH_2	2.26, m
4 b		1.39, d (6.3)		1.50, d (7.5)		1.36, m		1.74, m
5a	27.6, CH_2	1.72, m	27.9 CH_2	1.65, m	25.1, CH_2	1.88, ddd (15.3, 10.1, 5.0)	26.7, CH_2	2.09, m
5 b		1.37, m		1.49, d (7.5)		1.41, m		1.52, m
6	54.1, C		53.5, C		46.9, C		46.7, C	
7	164.3, C		110.9, C		81.8, C		148.3, C	
8a	95.7, CH	5.06, d (8.2)	61.9, CH_2	3.74, dd (9.2, 5.7)	204.8, C		31.0, CH_2	2.38, td (13.7, 4.7)
8 b								2.18, ddd (13.7, 4.7, 2.5)
9a	122.9, CH	5.48, ddd (11.4, 8.2, 2.4)	25.4, CH_2	1.85, m	122.7, CH	5.88, d (10.2)	32.6, CH_2	1.81, m
9 b				1.62, m				1.50, m
10a	123.8, CH	5.15, ddd (12.1, 7.2, 2.4)	36.9, CH_2	1.97, m	159.6, CH	6.51, d (10.2)	72.8, CH	4.24, dd (12.0, 4.7)
10 b				1.20, m				
11a	42.4, CH_2	2.40, d (19.1)	36.3, C		43.6, C		45.7, C	
11 b		1.82, dd (19.1, 7.2)						
12	32.5, C		23.5, CH_3	1.03, s	29.4, CH_3	1.25, s	11.3, CH_3	0.83, s
13a	23.3, CH_3	0.86, s	30.6, CH_3	0.92, s	25.0, CH_3	1.30, s	68.3, CH_2	3.86, d (11.2)
13 b								3.68, d (11.2)
14	27.1, CH_3	0.89, s	20.72, CH_3	1.57, s	27, CH_3	1.42, s	112.4, CH_2	4.49, s
15a	68.0, CH_2	3.40, d (11.1)			67.1, CH_2	3.47, d (11.3)	171.0, C	
15 b		3.21, m				3.70, d (11.3)		

[a] Measured in methanol-d_4.
[b] Measured in $CDCl_3$.

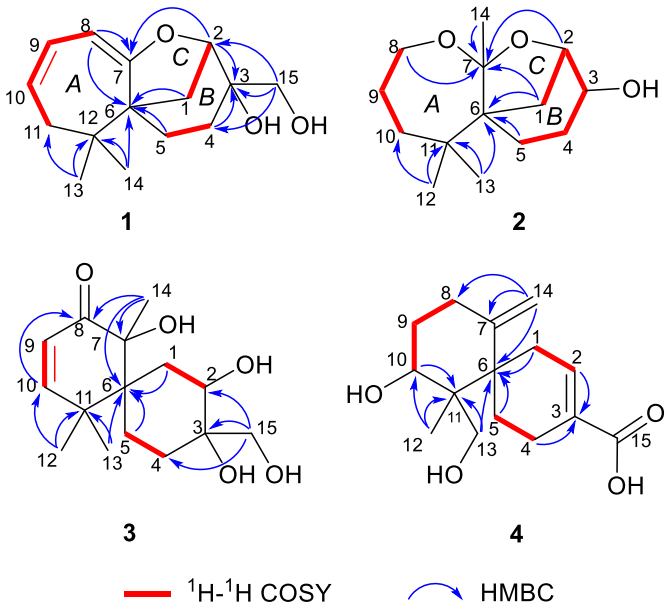

Fig. 2. Key 2D NMR correlations of compounds 1–4.

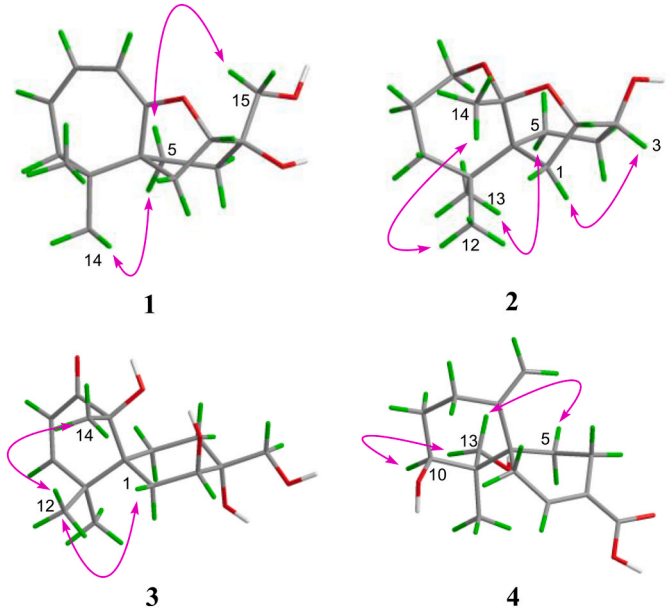

Fig. 3. Key ROESY correlations of compounds 1–4.

oxepane A was built. The same to 1, the HMBC correlations from H_2-1 and H_2-5 to C-6 constructed six-membered ring B, and the HMBC correlation from H-2 to C-7 established the furan C (Fig. 2). As shown in Fig. 3, the ROESY cross peaks of H_3-12/H_3-14 suggested that H_3-12 and H_3-14 were on the same side, which were assigned as β orientation randomly, while the ROESY cross peaks of H_3-13/H-5b suggested that H_3-13 and H-5b were α oriented. Based on these data, one ROESY correlation of H-3/H-1b suggested that the hydroxy at C-3 should be α oriented. The CD spectrum of 2 gives no Cotton effects since the structure has no chromophore, therefore, the absolute configuration was established by optical rotation calculations. As a result, the calculated data ([α] = + 83.2) for 2*S*,3*R*,6*S*,7*R*-2 matched with the experimental ones ([α] = + 29.2), which established the absolute configuration of 2. Thus, the structure of 2 was identified and named as steccherin B.

Compound 3 was obtained as a colorless oil. Its molecular formula $C_{15}H_{24}O_5$ was determined by HRESIMS (measured at *m/z* 307.15125 [M + Na]$^+$; calcd for $C_{15}H_{24}O_5Na^+$, 307.15214), corresponding to four degrees of unsaturation. The ^{1}H NMR spectrum of 3 exhibited three singlets for methyl groups at δ_H 1.25, 1.30 and 1.42, and two olefinic protons at δ_H 5.88 and 6.51. The ^{13}C NMR displayed fifteen signals which were classified as three CH_3, four CH_2, three CH, and five non-protonated carbons by DEPT experiment (Table 1). Analyses of the 1D NMR data indicated that 3 should possess a structure similar to that of acaciicolide K, a chamigrane sesquiterpene isolated from the fungus *Pseudolagarobasidium acaciicola* (Wibowo et al., 2016). Analyses of 2D NMR data indicated the only difference was that a hydroxy at C-2 in 3 replaced the ketone at C-2 in acaciicolide K, as supported by ^{1}H–^{1}H COSY correlations of H_2-1/H-2 and HMBC data (Fig. 2). In the ROESY spectrum, the cross peaks of H-1b/H_3-12 and H_3-12/H_3-14 suggested that H-1b, H_3-12 and H_3-14 were cofacial (Fig. 3). Finally, the experiment of single crystal X-ray diffraction determined the absolute configuration of 3 (Fig. 4). Thus, the structure of 3 was identified and named as steccherin C.

Compound 4 was obtained as a colorless oil. Its molecular formula $C_{15}H_{22}O_3$ was determined by HRESIMS (measured at *m/z* 289.14099 [M + Na]$^+$, calcd for $C_{15}H_{22}O_4Na^+$, 289. 14103), corresponding to five degrees of unsaturation. The ^{1}H NMR spectrum of 4 exhibited a singlet at δ_H 0.83 for a methyl group, and three olefinic protons at δ_H 4.24, 4.49 and 6.94. The ^{13}C NMR and DEPT data revealed one CH_3, seven CH_2, two CH, and five non-protonated carbons (Table 1). All spectroscopic data indicated that 4 was structurally similar to the known compound xylariterpenoid C, a chamigrane sesquiterpene from a Xylariaceae fungus (Wu et al., 2014). The only difference was that the methyl group of C-13 in xylariterpenoid C was oxidized to a hydroxymethylene in 4, which was confirmed by the HMBC correlations from H_2-13 to C-6, C-10, and C-11 (Fig. 2). In the ROESY spectrum, the cross peaks of H_2-13/H-5b and H-10/H_2-13 were observed, which indicated that H-10, H-5 and CH_2-13 were on the same side (assigned as α-orientation randomly), which led to an β-orientation for hydroxy at C-10 (Fig. 3). The absolute

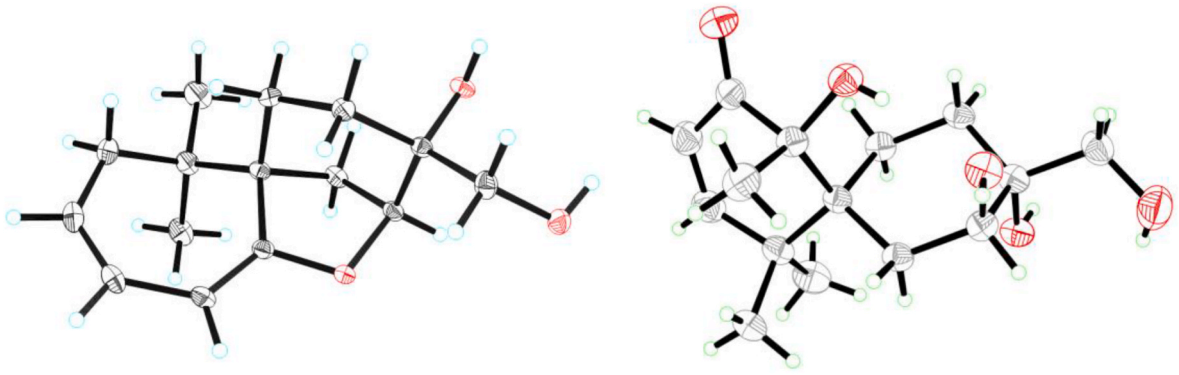

Fig. 4. ORTEP diagrams of 1 (left) and 3 (right) showing absolute configurations.

configuration of 4 was determined by ECD calculations, in which the calculated result for 4a has the same trends as the experimental data (Fig. 5). Therefore, the structure of 4 was identified and named as steccherin D.

Overall, four sesquiterpenes have been characterized from the fungus *S. ochraceum*. Of them, compounds 1 and 2 possessed previously undescribed carbon skeletons. Biogenetically, structures of 1 and 2 should be derived from normal chamigrane sesquiterpene by ring-rearrangement and ring-cleavage. As shown in Scheme 1, a possible pathway for the compounds 1–4 was given.

As introduced before, chamigrane-type sesquiterpenes have been proved to show good potential in inhibiting proliferation of lipopolysaccharide (LPS) induced B lymphocyte cells. Therefore, all compounds were tested for their in vitro inhibitory activities on concanavalin A (Con A)-induced T cell proliferation and LPS-induced B cell proliferation. The results (Table 2) indicated that compounds 1, 3, and 4 showed inhibitory activity against B lymphocyte cell proliferation, while compound 3 showed weak inhibition on T cell proliferation. In our previous study, the chamigrane dimer antroxazole A from *Antrodiella albocinnamomea* also showed good inhibition on B cell proliferation (He et al., 2022). All the data indicated that chamigrane-type sesquiterpenes may be potential candidates for selective B lymphocyte immunosuppressive agents.

3. Conclusions

In this study, four chamigrane sesquiterpenes have been isolated from the fungus *Steccherinum ochraceum* with structure identification and bioactivity test. Two compounds possessed previously undescribed carbon skeletons and three compounds displayed potent immunosuppressive activity. This study further disclosed the metabolites of the fungus *S. ochraceum* and provided the research basis for the further exploitation and utilization of chamigrane sesquiterpenes in immunosuppressive activity.

4. Experimental section

4.1. General experimental procedures

Melting points were obtained on an X-4 micro melting point apparatus. Optical rotations (OR) were measured with an Autopol IV polarimeter. Ultraviolet (UV) spectra were obtained using a double beam spectrophotometer UH5300. Infrared (IR) spectra were obtained by a Shimadzu IRTracer-100 spectrometer using KBr pellets. Circular dichroism (CD) spectra were recorded with an Applied Photophysics Chirascan-Plus CD Spectrometer. 1D and 2D NMR spectra were run on a Bruker Avance III 600 MHz spectrometer with TMS as an internal standard. High resolution electrospray ionization mass spectra (HR-ESIMS) were recorded on a LC-MS system consisting of a Q Exactive™ Orbitrap mass spectrometer using in ultra-high-resolution mode (140 000, at *m/z* 200). HREIMS spectra were recorded on a Waters AutoSpec Premier P776 mass spectrometer. Chemical shifts (δ) were expressed in ppm with references to TMS. X-ray crystallographic analysis was performed on a BRUKER D8 QUEST equipment. Column chromatography (CC) was carried out over silica gel (200–300 mesh), RP-18 gel (20–45 μm), and Sephadex LH-20. Medium-pressure liquid chromatography (MPLC) was performed on a Biotage One instrument. Preparative High Performance Liquid Chromatography (prep-HPLC) was performed on an Agilent 1260 series equipped with Zorbax SB- C18 columns (5 μm, 9.4 mm × 150 mm or 21.2 mm × 150 mm) and a diode array detector (DAD). Fractions were monitored by TLC (GF 254) or HPLC analysis.

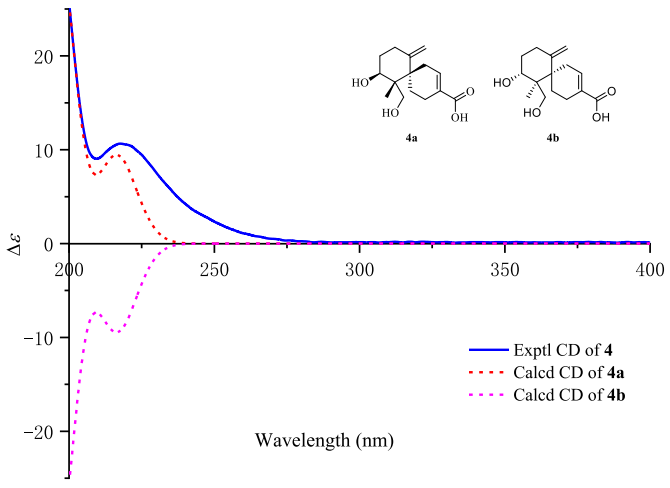

Fig. 5. ECD calculations for 4.

4.2. Fungal material

The fungus *Steccherinum ochraceum* (Pers.:Fr.) Gray. was collected from Yaoan county of Yunnan province, China (E101°12', N23°73'). It was identified based on internal transcribed spacer (ITS) sequence analysis and its morphology comparing with our previous sample (Liu, et al., 2010). The ITS sequence showed a 98% similarity to that of *Steccherinum ochraceum* (GenBank NO. JQ031130.1). The strain of *S. ochraceum* has been deposited at South-Central Minzu University with an access number of CGBWSHF-00106.

4.3. Fermentation condition

This strain was cultured on potato dextrose agar (PDA) medium at 24 °C for eight days when the mycelial biomass reached the maximum. It was used as "seeds" for further fermentation in rice medium. The rice medium was put into 400 mL bottles, each bottle contains 75 g rice and 100 mL water. All bottles with cultural media were put into a high-pressure sterilizing pot and sterilized at 120 °C for 25 min. Then, the "seeds" were cut into small pieces and transferred to each bottle. A total of 220 bottles were cultured at 25 °C for 30 days in a dark place.

4.4. Extraction and isolation

The culture of *S. ochraceum* (16 kg) was extracted six times with Me_2CO to afford an extract that was partitioned between water and EtOAc. The organic extract (60 g) was subjected to CC over silica gel (80−100 mesh) eluted with a gradient of $CHCl_3$–MeOH (from 1:0 to 0:1) to give five fractions A−E. Fraction B (9.5 g) was separated by MPLC over RP-18 column eluted with MeOH–H_2O (from 10:90 to 100:0, *v/v*) to give nine subfractions (B_1–B_9). Fraction B_4 (460 mg) was isolated by CC over silica gel eluted with petroleum ether (PE)-acetone (from 30:1 to 0:1, *v/v*) to give 1 (4 mg). Fraction B_7 (230 mg) was applied to Sephadex LH-20 eluting with MeOH, then the main fraction was prepared by HPLC with MeCN–H_2O (from 21:79 to 41:59 in 25 min, *v/v*, 4.0 mL/min) to obtain 2 (5.7 mg, retention time (t_R) = 18 min). Fraction C (12 g) was separated by MPLC over RP-18 column eluted with MeOH–H_2O (from 10:90 to 100:0, *v/v*) to give six subfractions (C_1–C_6). Fraction C_3 (720 mg) was separated by CC over silica gel with a gradient elution of PE-acetone (from 30:1 to 0:1) to afford eight subfractions ($C_{3\text{-}1}$−$C_{3\text{-}8}$). Fraction $C_{3\text{-}2}$ (180 mg) was subjected to Sephadex LH-20 eluted with MeOH, then the main section was isolated by HPLC (MeCN–H_2O from 13:87 to 33:67 in 25 min, *v/v*) to give 4 (9.8 mg, t_R = 14 min). Fraction $C_{3\text{-}5}$ (90 mg) was separated by CC over Sephadex LH-20 (MeOH), then isolated by HPLC (MeCN–H_2O from 17:83 to 37:63 in 25 min, *v/v*) to give 3 (6 mg, t_R = 19 min).

Steccherins A (1): Colorless crystals (MeOH), mp 138−142 °C; $[\alpha]_D^{25}$ + 99.2 (*c* 0.47, MeOH); UV (MeOH) λ_{max} (log ε) 205 (3.40), 275 (3.51) nm; ^{1}H NMR (600 MHz, methanol-d_4) and ^{13}C NMR (150 MHz, methanol-d_4) data, see Table 1; HRESIMS *m/z* 251.16414 $[M + H]^+$ (calcd for $C_{15}H_{23}O_3^+$, 251.16417).

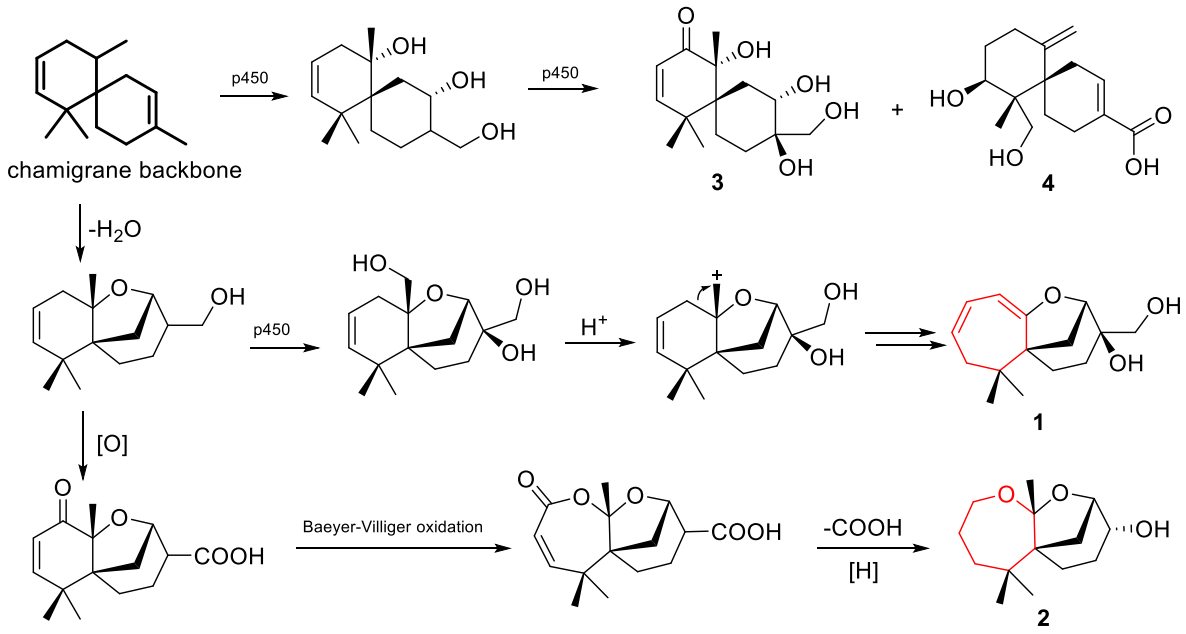

Scheme 1. Hypothesis for biogenetic pathway for 1–4.

Table 2
Data for 1–4 on T and B cell proliferation.

No.	ConA-induced T-cell proliferation	LPS-induced B-cell proliferation
	IC_{50} (μM)	IC_{50} (μM)
1	>40	26.3 ± 1.1
2	>40	>40
3	37.8 ± 1.3	6.2 ± 0.5
4	>40	16.1 ± 0.6
CsA	3.20 ± 0.02	0.13 ± 0.2

Steccherins B (2): Colorless oil; $[\alpha]_D^{25}$ + 29.2 (*c* 0.24, MeOH); IR (KBr) ν_{max} 3440, 2958, 2934, 1631, 1453, 1444, 1432, 1384, 1355, 1316, 1104, 1075, 1062 cm^{-1}; ^1H NMR (400 MHz, $CDCl_3$) and ^{13}C NMR (100 MHz, $CDCl_3$) data, see Table 1; HREIMS *m/z* 240.1728 $[M]^+$ (calcd for $C_{14}H_{24}O_3$, 240.1725).

Steccherins C (3): Colorless crystals (MeOH), mp 166−171 °C; $[\alpha]_D^{25}$ + 10.5 (*c* 0.41, MeOH); UV (MeOH) λ_{max} (log ε) 225 (3.91) nm; ^1H NMR (600 MHz, methanol-d_4) and ^{13}C NMR (150 MHz, methanol-d_4) data, see Table 1; HRESIMS *m/z* 307.15146 $[M + Na]^+$ (calcd for $C_{15}H_{24}O_5Na^+$, 307.15159).

Steccherins D (4): Colorless oil; $[\alpha]_D^{25}$ + 64.6 (*c* 0.54, MeOH); UV (MeOH) λ_{max} (log ε) 215 (3.70) nm; ^1H NMR (600 MHz, methanol-d_4) and ^{13}C NMR (150 MHz, methanol-d_4) data, see Table 1; HRESIMS *m/z* 289.14099 [M + Na]+(calcd for $C_{15}H_{22}O_4Na^+$, 289. 14103).

4.5. X-ray crystallographic analysis

X-Ray crystallographic data for 1: $C_{15}H_{22}O_3$, $M = 250.32$, $a = 8.3855(4)$ Å, $b = 10.4681(5)$ Å, $c = 30.3160(16)$ Å, $\alpha = 90°$, $\beta = 90°$, $\gamma = 90°$, $V = 2661.1(2)$ Å^3, $T = 150(2)$ K, space group *P*212121, $Z = 8$, μ(Cu Kα) = 0.684 mm^{-1}. A total of 19339 reflections were measured, in which 4939 were independent reflections ($R_{int} = 0.0647$). The R_1 value was 0.0485 ($I > 2\sigma(I)$). The final $wR(F^2)$ value was 0.1539 ($I > 2\sigma(I)$). The final R_1 value was 0.0510 (all data). The final $wR(F^2)$ value was 0.1559 (all data). The goodness of fit on F^2 was 1.147. Flack parameter was 0.15(7). The data (cif file) have been deposited at Cambridge Crystallographic Data Centre (www.ccdc.cam.ac.uk) with a CCDC number of 2259196.

X-Ray crystallographic data for 3: $C_{30}H_{48}O_{10}$, $M = 568.68$, $a = 6.6543(6)$ Å, $b = 9.9784(9)$ Å, $c = 10.6672(10)$ Å, $\alpha = 89.595(4)°$, $\beta = 88.509(4)°$, $\gamma = 88.757(4)°$, $V = 707.87(11)$ Å3, $T = 300(2)$ K. space group *P*1, $Z = 1$, μ(Cu Kα) = 1.54178 mm^{-1}. A total of 28371 reflections were measured, in which 5746 were independent reflections ($R_{int} = 0.0708$). The R_1 value was 0.0580 ($I > 2\sigma(I)$). The final $wR(F^2)$ value was 0.1545 ($I > 2\sigma(I)$). The final R_1 value was 0.0665 (all data). The final $wR(F^2)$ value was 0.1634 (all data). The goodness of fit on F^2 was 1.040. The Flack parameter was 0.40(12). The data (cif file) have been deposited at Cambridge Crystallographic Data Centre (www.ccdc.cam.ac.uk) with a CCDC number of 2259198.

4.6. Optical rotation calculations

Conformation search based on molecular mechanics with MMFF force fields were performed for 2a and 2 b gave six stable conformers with populations higher than 1%. The optical rotation calculations were carried out using the Gaussian 16 software package (M. J. Frisch et al., 2016). The optical rotations were calculated at the pAPFD/6–311++G (2 d, 2p) level in chloroform with the PCM model. For details, see Supporting Information (Section S2).

4.7. ECD calculations

Conformation search based on molecular mechanics with MMFF force fields were performed for 4a and 4 b gave twelve stable conformers with populations higher than 1%. The ECD calculations were carried out using the Gaussian 16 software package. The ECD were calculated at the mPW1PW91/6-311 + G(d,p) level in methanol with the PCM model. The ECD curves were simulated in SpecDis V1.71 using a Gaussian function (Bruhn et al., 2013). For details, see Supporting Information (Section S1).

4.8. Immunosuppressive assay

The assay was carried out by Shanghai Institute of Materia Medica, Chinese Academy of Sciences, using the method we reported in previous publications (He et al., 2022; Liang et al., 2021; Wang et al., 2020). The details were afforded in Supporting Information.

Declaration of competing interest

The corresponding authors, on behalf of all authors of the manuscript, disclose that there is no potential competing or non-financial interest.

Data availability

Data will be made available on request.

Acknowledgments

This work was financially supported by the National Natural Science Foundation of China (21961142008 and 22177138) and the Fundamental Research Funds for the Central Universities, South-Central Minzu University (CZP21001).

Appendix A. Supplementary data

Supplementary data to this article can be found online at https://doi.org/10.1016/j.phytochem.2023.113830.

References

Bruhn, T., Schaumlöffel, A., Hemberger, Y., Bringmann, G., 2013. SpecDis: quantifying the comparison of calculated and experimental electronic circular dichroism spectra. Chirality 25, 243–249. https://doi.org/10.1002/chir.22138.

Conrado, R., Gomes, T.C., Roque, G.S., De Souza, A.O., 2022. Overview of bioactive fungal secondary metabolites: cytotoxic and antimicrobial compounds. J. Antibiot. 11 https://doi.org/10.3390/antibiotics11111604.

Edner, N.M., Carlesso, G., Rush, J.S., Walker, L.S.K., 2020. Targeting co-stimulatory molecules in autoimmune disease. Nat. Rev. Drug Discov. 19, 860–883. https://doi.org/10.1038/s41573-020-0081-9.

Frisch, M.J., G W T, Schlegel, H.B., Scuseria, G.E., Robb, M.A., Cheeseman, J.R., Scalmani, G., Barone, V., Petersson, G.A., Nakatsuji, H., Li, X., Caricato, M., Marenich, A.V., Bloino, J., Janesko, B.G., Gomperts, R., Mennucci, B., Hratchian, H. P., Ortiz, J.V., Izmaylov, A.F., Sonnenberg, J.L., Williams-Young, D., Ding, F., Lipparini, F., Egidi, F., Goings, J., Peng, B., Petrone, A., Henderson, T., Ranasinghe, D., Zakrzewski, V.G., Gao, J., Rega, N., Zheng, G., Liang, W., Hada, M., Ehara, M., Toyota, K., Fukuda, R., Hasegawa, J., Ishida, M., Nakajima, T., Honda, Y., Kitao, O., Nakai, H., Vreven, T., Throssell, K., Montgomery Jr., J.A., Peralta, J.E., Ogliaro, F., Bearpark, M.J., Heyd, J.J., Brothers, E.N., Kudin, K.N., Staroverov, V.N., Keith, T.A., Kobayashi, R., Normand, J., Raghavachari, K., Rendell, A.P., Burant, J. C., Iyengar, S.S., Tomasi, J., Cossi, M., Millam, J.M., Klene, M., Adamo, C., Cammi, R., Ochterski, J.W., Martin, R.L., Morokuma, K., Farkas, O., Foresman, J.B., Fox, D.J., 2016. Gaussian, vol. 16. Gaussian, Inc., Wallingford CT.

Grossart, H.P., Van den Wyngaert, S., Kagami, M., Wurzbacher, C., Cunliffe, M., Rojas-Jimenez, K., 2019. Fungi in aquatic ecosystems. Nat. Rev. Microbiol. 17, 339–354. https://doi.org/10.1038/s41579-019-0175-8.

He, J., Yu, W.W., Isaka, M., Cox, R.J., Liu, J.K., Feng, T., 2022. Antroxazole A, an oxazole-containing chamigrane dimer from the fungus Antrodiella albocinnamomea with immunosuppressive activity. Org. Biomol. Chem. 20, 7278–7283. https://doi.org/10.1039/D2OB01443B.

Hridoy, M., Gorapi, M.Z., Noor, S., Chowdhury, N.S., Rahman, M.M., Muscari, I., Masia, F., Adorisio, S., Delfino, D.V., Mazid, M.A., 2022. Putative anticancer compounds from plant-derived endophytic fungi: a review. Molecules 27. https://doi.org/10.3390/molecules27010296.

Hyde, K.D., Xu, J., Rapior, S., Jeewon, R., Lumyong, S., Niego, A.G.T., Abeywickrama, P. D., Aluthmuhandiram, J.V.S., Brahamanage, R.S., Brooks, S., Chaiyasen, A., Chethana, K.W.T., Chomnunti, P., Chepkirui, C., Chuankid, B., de Silva, N.I., Doilom, M., Faulds, C., Gentekaki, E., Gopalan, V., Kakumyan, P., Harishchandra, D., Hemachandran, H., Hongsanan, S., Karunarathna, A., Karunarathna, S.C., Khan, S., Kumla, J., Jayawardena, R.S., Liu, J.K., Liu, N., Luangharn, T., Macabeo, A.P.G., Marasinghe, D.S., Meeks, D., Mortimer, P.E., Mueller, P., Nadir, S., Nataraja, K.N., Nontachaiyapoom, S., O'Brien, M., Penkhrue, W., Phukhamsakda, C., Ramanan, U. S., Rathnayaka, A.R., Sadaba, R.B., Sandargo, B., Samarakoon, B.C., Tennakoon, D. S., Siva, R., Sriprom, W., Suryanarayanan, T.S., Sujarit, K., Suwannarach, N., Suwunwong, T., Thongbai, B., Thongklang, N., Wei, D., Wijesinghe, S.N., Winiski, J., Yan, J., Yasanthika, E., Stadler, M., 2019. The amazing potential of fungi: 50 ways we can exploit fungi industrially. Fungal Divers. 97, 1–136. https://doi.org/10.1007/s13225-019-00430-9.

Liang, D.D., Yi, X.W., Wu, H., Li, Z.H., Wang, G.K., Cheng, G.G., Feng, T., 2021. Antrodillin, an immunosuppressive sesquiterpenoid from higher fungus Antrodiella albocinnamomea. RSC Adv. 11, 1124–1127. https://doi.org/10.1039/D0RA10055B.

Liu, D.Z., Luo, M.H., 2010. Two new chamigrane metabolites from fermentation broth of Steccherinum ochraceum. Fitoterapia 81, 1205–1207. https://doi.org/10.1016/j.fitote.2010.08.004.

Liu, D.Z., Dong, Z.J., Wang, F., Liu, J.K., 2010. Two novel norsesquiterpene peroxides from basidiomycete Steccherinum ochraceum. Tetrahedron Lett. 51, 3152–3153. https://doi.org/10.1016/j.tetlet.2010.04.048.

Moiseenko, K.V., Glazunova, O.A., Shakhova, N.V., Savinova, O.S., Vasina, D.V., Tyazhelova, T.V., Psurtseva, N.V., Fedorova, T.V., 2019. Fungal adaptation to the advanced stages of wood decomposition: insights from the Steccherinum ochraceum. Microorganisms 7. https://doi.org/10.3390/microorganisms7110527.

Ortega, H.E., Torres-Mendoza, D., Caballero, E.Z., Cubilla-Rios, L., 2021. Structurally uncommon secondary metabolites derived from endophytic fungi. J. Fungi 7. https://doi.org/10.3390/jof7070570.

Pusztahelyi, T., Holb, I., Pócsi, I., 2015. Secondary metabolites in fungus-plant interactions. Front. Plant Sci. 6 https://doi.org/10.3389/fpls.2015.00573.

Ramalingam, S., Shah, A., 2021. Stem cell therapy as a treatment for autoimmune disease—updates in lupus, scleroderma, and multiple sclerosis. Curr. Allergy Asthma Rep. 21, 22. https://doi.org/10.1007/s11882-021-00996-y.

Rose, N.R., 2016. Prediction and prevention of autoimmune disease in the 21st century: a review and preview. Am. J. Epidemiol. 183, 403–406. https://doi.org/10.1093/aje/kwv292.

Rustamova, N., Bozorov, K., Efferth, T., Yili, A., 2020. Novel secondary metabolites from endophytic fungi: synthesis and biological properties. Phytochemistry Rev. 19, 425–448. https://doi.org/10.1007/s11101-020-09672-x.

Singh, A., Singh, D.K., Kharwar, R.N., White, J.F., Gond, S.K., 2021. Fungal endophytes as efficient sources of plant-derived bioactive compounds and their prospective applications in natural product drug discovery: insights, avenues, and challenges. Microorganisms 9. https://doi.org/10.3390/microorganisms9010197.

Wang, M., Du, J.X., Hui Xiang, Y., Dai, Q., Liu, Y.P., He, J., Wang, Y., Li, Z.H., Feng, T., Liu, J.-K., 2020. Sesquiterpenoids from cultures of the basidiomycetes Irpex lacteus. J. Nat. Prod. 83, 1524–1531. https://doi.org/10.1021/acs.jnatprod.9b01177.

Wang, H.N., Sun, S.S., Liu, M.Z., Yan, M.C., Liu, Y.F., Zhu, Z., Zhang, Z., 2022. Natural bioactive compounds from marine fungi (2017–2020). J. Asian Nat. Prod. Res. 24, 203–230. https://doi.org/10.1080/10286020.2021.1947254.

Wibowo, M., Prachyawarakorn, V., Aree, T., Mahidol, C., Ruchirawat, S., Kittakoop, P., 2016. Cytotoxic sesquiterpenes from the endophytic fungus Pseudolagarobasidium acaciicola. Phytochemistry 122, 126–138. https://doi.org/10.1016/j.phytochem.2015.11.016.

Wu, Z.Y., Wu, Y., Chen, G.D., Hu, D., Li, X.X., Sun, X., Guo, L.D., Li, Y., Yao, X.S., Gao, H., 2014. Xylariterpenoids A–D, four new sesquiterpenoids from the Xylariaceae fungus. RSC Adv. 4, 54144–54148. https://doi.org/10.1039/C4RA10365C.

Zhao, Z.Z., Feng, W.S., Liang, X.B., Xue, G.M., Si, Y.Y., Chen, H.P., Liu, J.K., 2019. Ochracines A-E, chamigrane-related norsesquiterpene derivatives from the basidiomycete Steccherinum ochraceum HFG119. Fitoterapia 139, 104362. https://doi.org/10.1016/j.fitote.2019.104362.

Zhao, Z.Z., Zhao, Q.L., Feng, W.S., He, H.R., Li, M., Xue, G.M., Chen, H.P., Liu, J.-K., 2021. Structure and absolute configuration assignments of ochracines F–L, chamigrane and cadinane sesquiterpenes from the basidiomycete Steccherinum ochraceum HFG119. RSC Adv. 11, 18693–18701. https://doi.org/10.1039/D1RA03320D.